Molecular Effects in Beam-Foil Electron Transfer to the Continuum

V. H. Ponce, E. González Lepera, W. Meckbach, and I. B. Nemirovsky
Centro Atómico Bariloche, Comisión Nacional de Energía Atómica, Instituto Balseiro, Universidad Nacional de Cuyo, 8400 Bariloche, Argentina
(Received 9 January 1981)

Distributions of electrons emitted when thin carbon foils are bombarded with H^+ and H_2^+ ion beams are measured along the forward direction and close to the projectile velocity. The ratio between electron yields per proton for H_2^+ and H^+ projectiles grows from unity away from the electron peak to a maximum at the peak. This explains the narrower peak widths observed for molecular projectiles. The results are interpreted in terms of a correlated action of the emergent protons on the process of electron transfer to the continuum.

PACS numbers: 34.70.+e, 34.50.Hc, 79.20.Rf

The use of molecular projectiles in beam-foil electron transfer to the continuum (ETC) has given indication of an overall electron-yield enhancement: Dettmann, Harrison, and Lucas[1] report similar electron spectra for equal-velocity H_2^+ and H^+ projectiles, but the yield per proton is higher by a factor of 2 for H_2^+. Duncan and Menéndez[2] find narrower single angular distributions for incident H_2^+, but obtain the same yield for both types of projectiles. Meckbach *et al.*[3] also find narrower peaks for longitudinal and transverse electron spectra.

In this work we compare the doubly differential electron distributions along the forward direction for single protons and hydrogen molecular ions of equal velocity. Carbon foils of 2^{+2}_{-1} and 5^{+3}_{-2} $\mu g/cm^2$ thickness, as specified by the manufacturer,[4] have been bombarded with H^+ and H_2^+ projectiles of 70 and 100 keV/u. The point of emergence of the beam is on the focus of a coaxial cylindric electrostatic analyzer, whose relative velocity resolution is $R_v = 0.0004$ and aperture of angular acceptance is $\theta_0 = 0.000\,29$ rad. The resulting pairs of spectra and their quotients Q are represented in Fig. 1. It is confirmed that the cusps measured for correlated $2H^+$ projectiles are narrower than those obtained with single H^+. We observe that at their wings the spectra tend to become identical, whereas close to the maximum of the peaks, where the electron and ion velocities tend to coincide, the counting yields obtained with molecular fragments are larger than those obtained with individual protons. As the electron counts per channel are normalized to the beam charge emerging from the target, these results can be attributed to the fact that correlated protons are more effective than single protons in the production of ETC electrons. This is made evident in the spectra that result for the quotient Q: At the wings $Q = Q_c$ becomes constant and very close to unity.[5] When the electron velocity approaches the projectile velocity, Q exhibits a maximum, Q_p, which can be considered as a direct measure for the increased effectiveness of correlated molecular fragments for the ETC process.

There are two processes that may be responsible for the production of ETC electrons for solid targets: electron capture to the continuum of the projectile from the last atomic layer of the foil,[1] and electron loss to the continuum from electronic states carried along by the projectile as it emerges from the foil.[6,7] We now proceed to consider electron capture to the continuum of a projectile formed by a pair of correlated charges emerging from a solid foil.

We assume a single electron e bound to the target 2 and approximate the transition amplitude by the second-order Born approximation, evaluated to leading order in the collision velocity. Let $\vec{r}_2, \vec{R}_2$ to be relative coordinates for the pairs $(2, e)$ and $(2+e, 2H^+)$, respectively, while $\vec{r}_1, \vec{R}_1$ are those between $(2H^+, e)$ and $(2, 2H^+ + e)$. $\vec{R}$ is the coordinate between protons in $2H^+$, assumed to be invariant through the collision. The momenta associated with coordinates $(\vec{r}_1, \vec{r}_2, \vec{R}_1, \vec{R}_2)$ are $(\vec{\kappa}_1, \vec{\kappa}_2, \vec{K}_f^1, \vec{K}_f^2)$, respectively. Initial and final scattering states are

$$\chi_i = \exp(i\vec{K}_i \cdot \vec{R}_2)\varphi_i(\vec{r}_2),$$
$$\chi_f = \exp(i\vec{K}_f^{\,1} \cdot \vec{R}_1)\exp(i\vec{\kappa}_1 \cdot \vec{r}_1)\varphi_{\vec{\kappa}_1}(\vec{r}_1, \vec{R}), \quad (1)$$

where the final electron state $\exp(i\vec{\kappa}_1 \cdot \vec{r}_1)\varphi_{\vec{\kappa}_1}(\vec{r}_1, \vec{R})$ may be expressed as a combination of the usual molecular eigenstates of the electronic angular momentum along $\vec{R}$ and the operator of inversion of $\vec{r}_1$, with the same energy eigenvalue $E = \kappa_1^2/2$.

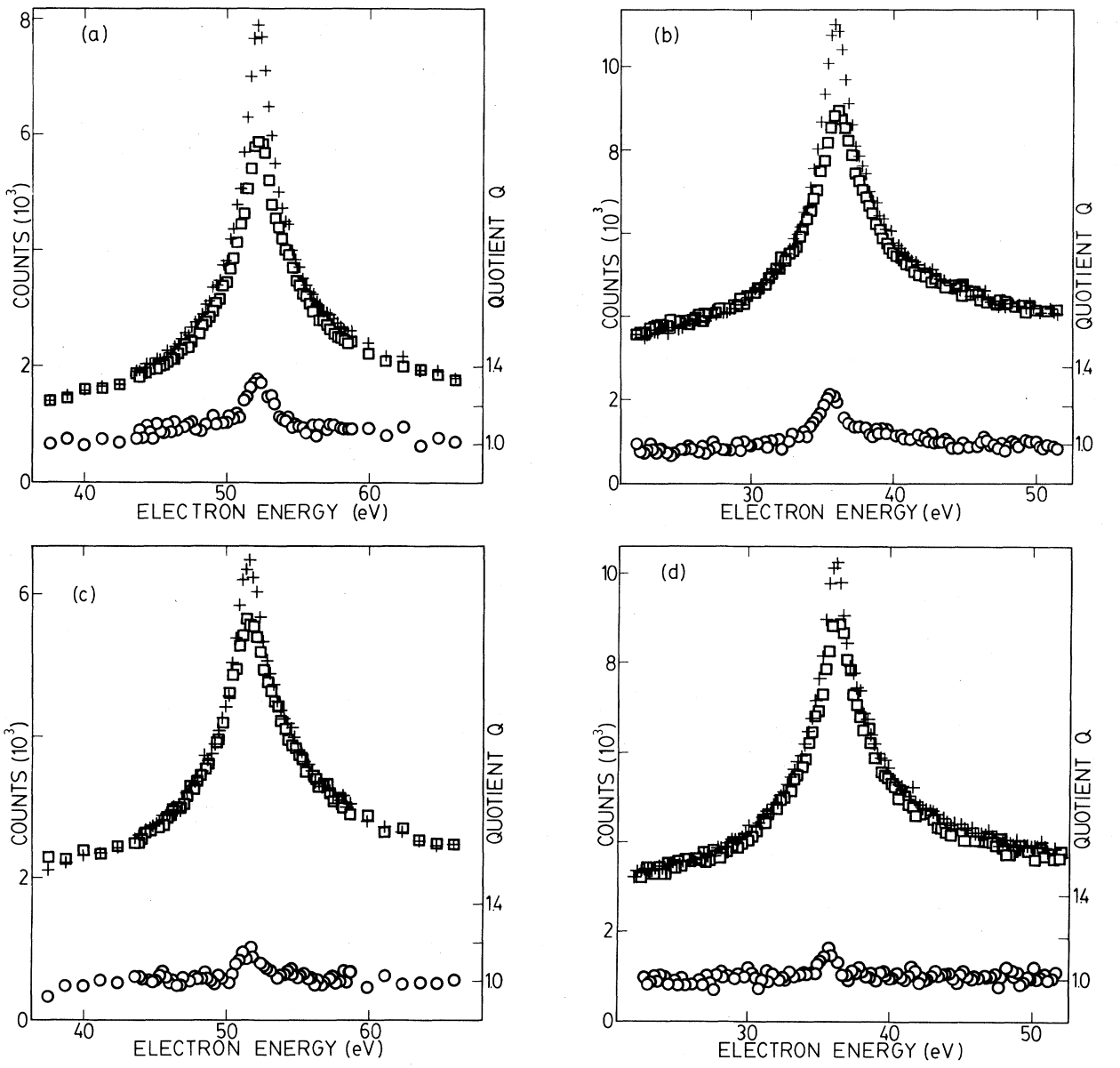

FIG. 1. Measured double-differential electron distributions per unit beam charge for incident H_2^+ (plusses) and H^+ (squares) projectiles and their quotients Q (circles). R is the interproton distance upon emergence from the foil that results for incident H_2^+. (a) $v = 2.00$ a.u. (100 keV/u), 2-μg/cm^2 carbon foil, $R = 2.4$ a.u. (b) $v = 1.67$ a.u. (70 keV/u), 2-μg/cm^2 carbon foil, $R = 2.5$ a.u. (c) $v = 2.00$ a.u. (100 keV/u), 5-μg/cm^2 carbon foil, $R = 3.9$ a.u. (d) $v = 1.67$ a.u. (70 keV/u), 5-μg/cm^2 carbon foil, $R = 4.6$ a.u.

The second-order Born transition amplitude is

$$T_{i,\vec{\kappa}_1}(2H^+, \vec{R}) = \langle \chi_f | V_1 | \chi_i \rangle + \langle \chi_f | V_2 G_0{}^+ V_1 | \chi_i \rangle. \quad (2)$$

Here

$$V_1 = V(\vec{r}_1 - \vec{R}/2) + V(\vec{r}_1 + \vec{R}/2), \quad V(\vec{x}) = -Z/x, \quad (3)$$

and V_2 is the potential of the residual target.

The presence of the displacements $\pm \vec{R}/2$ in the argument of V in (3) adds a phase $\exp(\pm i \vec{k} \cdot \vec{R}/2)$ to the Fourier transform $\tilde{V}(\vec{k})$, defined through $\tilde{f}(\vec{k}) = \int d^3r \exp(-i\vec{k} \cdot \vec{r}) f(\vec{r})$. Therefore, using the results for the case of a single charge as projectile,[8] we obtain

$$T_{i,\vec{\kappa}_1}(2H^+, \vec{R}) = I(\vec{R}/2) + I(-\vec{R}/2) \quad (4)$$

with

$$I(\pm\vec{R}/2) = (2\pi)^{-3}\tilde{\varphi}_i(-\vec{K})\int d^3k\,\tilde{\varphi}_{\vec{\kappa}_1}{}^*(\vec{k},\vec{R})\,\tilde{V}(\vec{P}-\vec{k})\exp[\pm i(\vec{P}-\vec{k})\vec{R}/2]$$
$$+(2\pi)^{-6}\int d^3k\,d^3k'\,\tilde{\varphi}_{\vec{\kappa}_1}{}^*(\vec{k},\vec{R})\tilde{V}_2(\vec{K},\vec{k}')G_0{}^+(\vec{k},\vec{k}')\tilde{V}(\vec{P}-\vec{k})\exp[\pm i(\vec{P}-\vec{k})\vec{R}/2]\,\tilde{\varphi}_i(\vec{k}'), \quad (5)$$

where $\vec{P}=\vec{K}_i-\vec{K}_f{}^2=\vec{K}_i-\vec{K}_f{}^1-\vec{\kappa}_1$ is the momentum transferred by the projectile, and $\vec{K}=\vec{\kappa}_2-\vec{P}$. Since $K\sim P\gtrsim v/2$ for a charge transfer process, we may extract the potentials from the integrals (5) if we settle for determining only the leading term in an expansion in powers of v^{-1}. This "peaking approximation"[1,9] eliminates part of the contributions in the following orders; therefore only the leading term of $G_0{}^+$ needs to be considered in (5):

$$G_0{}^+(\vec{k},\vec{k}')^{-1}\cong D_0+(\vec{P}-\vec{v})\vec{k}-\vec{P}\cdot\vec{k}', \quad (6)$$

where $D_0=-P^2/2+\vec{v}\cdot\vec{P}$. For the $\vec{k},\vec{k}'$ values relevant to the integral (5) $G_0{}^+$ behaves as v^{-2} except at the region of the critical angle ($D_0\cong 0$) where it is of order v^{-1}. Using the peaking approximation and substituting (6) into (5) we obtain for (4), to leading order in v and outside the critical-angle region,

$$T_{i,\vec{\kappa}_1}(2H^+,\vec{R}) = T_{i,\vec{\kappa}_1}(H^+)[\,\varphi_{\vec{\kappa}_1}(-\vec{R}/2,\vec{R})e^{i\vec{P}\cdot\vec{R}/2}+\varphi_{\vec{\kappa}_1}(\vec{R}/2,\vec{R})e^{-i\vec{P}\cdot\vec{R}/2}]/f_C{}^*(Z/K_1), \quad (7)$$

where

$$T_{i,\vec{\kappa}_1}(H^+) = (2\pi)^{-3}f_C{}^*(Z/\kappa_1)\tilde{V}_1(P)|\,\tilde{\varphi}_i(-\vec{K})+(2\pi)^{-3}\tilde{V}_2(\vec{K})\varphi_i(0)D_0{}^{-1}| \quad (8)$$

is the second-order Born amplitude for a single projectile H^+ to leading order in v^{-1}, with the Coulomb factor f_C representing the value of the continuum orbital at the proton position.

A complete study of terms of following orders in v^{-1}, which includes anisotropic contributions to the electron distribution, requires that one keeps the potentials inside the momentum-space integrals in (5); it is then seen[10] that the v^{-1} expansion converges rather slowly for not too large collision velocities.

The triple-differential cross section is proportional to the square of (8); the double-differential cross section Σ is obtained by integrating the former over the allowed momentum transfers $\vec{P}$ where, consistent with the peaking approximation, we neglect the crossed term $2|\varphi_{\vec{\kappa}_1}{}^*(-\vec{R}/2,\vec{R})\varphi_{\vec{\kappa}_1}(\vec{R}/2,\vec{R})|\times\cos\vec{P}\cdot\vec{R}$ because $\vec{P}\cdot\vec{R}\gg 1$ and should produce a negligible contribution when integrated over $\vec{P}$ or averaged over $\hat{R}$:

$$\Sigma_{i,\vec{\kappa}_1}(2H^+,\vec{R}) = \Sigma_{i,\vec{\kappa}_1}(H^+)[\,|\varphi_{\vec{\kappa}_1}(\vec{R}/2,\vec{R})|^2+|\varphi_{\vec{\kappa}_1}(-\vec{R}/2,\vec{R})|^2]/|f_C(Z/\kappa_1)|^2. \quad (9)$$

Summing over the random molecular orientations $\hat{R}$ in the incident beam yields

$$\Sigma_{i,\vec{\kappa}_1}(2H^+,\vec{R}) = 2\Sigma_{i,\vec{\kappa}_1}(H^+)\,|\bar{\varphi}_{\vec{\kappa}_1}(R/2,R)/f_C(Z/\kappa_1)|^2. \quad (10)$$

Because of the relative orientation of $\vec{R}$ with respect to $\vec{\kappa}_1$, the function φ depends effectively on $\vec{R}\cdot\vec{\kappa}_1$, and consequently the average $\bar{\varphi}$ appears in (10). The term $|\bar{\varphi}_{\vec{\kappa}_1}/f_C|^2$ represents the influence of the correlation between projectiles on the electron distribution Σ, whose dominant $\vec{\kappa}_1$ dependence originates from $|\bar{\varphi}_{\vec{\kappa}_1}(R/2,R)|^2$ which can be viewed as a normalization factor of the continuum orbital adjusted to have an asymptotic plane wave in the momentum scale.

Let us now see if equivalent effects are also present for electron loss from states that may accompany a correlated pair of protons: Now the initial electron state in (1) is a bound orbital $\varphi_i(\vec{r}_1,\vec{R})$ and the perturbation is the target potential $V_2(\vec{r}_2)$. Neglecting target excitation, the first-order Born transition amplitude results in[6]

$$T_{i,\vec{\kappa}_1}(2H^+,\vec{R}) = \tilde{V}_2(\vec{P})\int d^3r_1\,\varphi_{\vec{\kappa}_1}{}^*(\vec{r}_1,\vec{R})\exp[i(\vec{P}-\vec{\kappa}_1)\vec{r}_1]\,\varphi_i(\vec{r}_1,\vec{R}). \quad (11)$$

Here the dominant dependence on $\vec{\kappa}_1$ can also be extracted from the integral as a factor $\bar{\varphi}_{\vec{\kappa}_1}(R/2,R)$; therefore the electron distribution Σ coming from the electron loss to the continuum will also exhibit the correlation effects already found for electron capture to the continuum. Because of the R dependence of the initial state φ_i in (11), the factor multiplying $|\bar{\varphi}_{\vec{\kappa}_1}(R/2,R|^2$ for electron loss may be different for correlated pairs $2H^+$ as compared with single projectiles H^+, contrary to what occurred for electron capture to the continuum.

A continuum atomic orbital has a wavelength that asymptotically is $2\pi/\kappa_1$; at finite distances from the nucleus it will be smaller because of

the presence of the attractive potential. When many of these wavelengths are contained in the interproton distance R, we may expect that the electron wave function around each proton is not much influenced by the other proton and close to the nuclei it may be approximated by the atomic orbitals centered on them. The correlation term in (10) is then equal to 1, and (10) satisfies the obvious condition that the cross section for a projectile composed of two uncorrelated protons is twice that for a single proton.

When the internuclear distance R is not large compared with the wavelength, $\overline{\varphi}_{\kappa_1}^{\rightarrow}(R/2, R)$ presents molecular characteristics and differs from $f_C(Z/\kappa_1)$. The local wavelength close to the protons is of order π/Z, and so for $R \ll \pi/Z$ the electron sees a unified charge of value $2Z$ and $\overline{\varphi}_{\kappa_1}^{\rightarrow}(R/2, R) \simeq f_C(2Z/\kappa_1)$. Then the correlation factor, close to the peak of the electron distribution, which means $\kappa_1 \ll Z$, is

$$|\overline{\varphi}_{\kappa_1}^{\rightarrow}(R/2, R)/f_C(Z/\kappa_1)|^2 \cong 2,$$

when $R \ll \pi/Z$.

We conclude that the ratio between the electron distributions carried by $2H^+$ and H^+ is bound between the values 1 and 2; furthermore, the larger the interproton distance R, the smaller the enhancement of the distribution around $2H^+$ compared with that of H^+. These two features are verified by our measurements.

If we analyze the correlation factor for a fixed R we see that for increasing κ_1 the electronic wavelength decreases and we reach, away from the peak, the region where the electron behaves as in an atomic state around each proton; the correlation factor there is equal to 1. This region is reached for smaller κ_1 when R is increased, and again the experimental results of Fig. 1 verify this feature of the theory.

[1]K. Dettmann, K. G. Harrison, and M. W. Lucas, J. Phys. B 7, 269 (1974).

[2]M. M. Duncan and M. G. Menéndez, Phys. Rev. A 13, 566 (1976).

[3]W. Meckbach, K. C. R. Chiu, H. H. Brongersma, and J. Wm. McGowan, J. Phys. B 10, 3255 (1977).

[4]Yissum Research Development Co., Jerusalem, Israel.

[5]Our electron-counting normalization did not account for the slight difference in beam-foil charge distributions obtained with incident H^+ and H_2^+ as reported by B. T. Meggit, K. G. Harrison, and M. W. Lucas, J. Phys. B 6, L362 (1973).

[6]F. Drepper and J. S. Briggs, J. Phys. B 9, 2063 (1976).

[7]I. A. Sellin, J. Phys. (Paris), Colloq. 40, C1-225 (1979); V. H. Ponce and W. Meckbach, Comments At. Mol. Phys. 10, 231 (1981); W. Brandt and R. H. Ritchie, Phys. Lett. 62A, 374 (1974); M. H. Day, Phys. Rev. Lett. 44, 752 (1980).

[8]J. E. Miraglia and V. H. Ponce, J. Phys. B 13, 1195 (1980).

[9]K. Dettmann, in *Springer Tracts in Modern Physics 58* (Springer, Berlin, 1971), p. 119.

[10]V. H. Ponce, to be published.

Stabilizing Effect of Finite-Gyroradius Beam Particles on the Tilting Mode of Spheromaks

R. N. Sudan

Laboratory of Plasma Studies, Cornell University, Ithaca, New York 14853

and

P. K. Kaw

Plasma Physics Laboratory, Princeton University, Princeton, New Jersey 08540

(Received 29 December 1980)

The equilibrium shape of a low-pressure spheromak plasma with a small component of toroidal current carried by finite-gyroradius particles is computed. The stabilizing influence of this current on the tilting mode is determined by employing an energy principle that includes gyroscopic and finite-gyroradius effects.

PACS numbers: 52.55.-s, 52.20.Dq, 52.35.Py

The favorable characteristics of nearly force-free, spherical magnetic configurations[1] dubbed "spheromaks" have led to an enthusiastic vision of a fusion reactor[2] with engineering advantages superior to that of tokamaks. However, Rosenbluth and Bussac[3] have shown that these configura-

